

Cusps in the quenched dynamics of a Bloch state

J. M. Zhang

*Fujian Provincial Key Laboratory of Quantum Manipulation and New Energy Materials,
College of Physics and Energy, Fujian Normal University, Fuzhou 350007, China*

We report some nonsmooth dynamics of a Bloch state in a one-dimensional tight binding model. After a sudden change of the potential of some site, quantities like the survival probability of the particle in the initial Bloch state show cusps periodically. This phenomenon is a nonperturbative counterpart of the nonsmooth dynamics observed previously (Zhang and Haque, arXiv:1404.4280) in the tight binding model. We explain it by exactly solving a truncated and linearized model.

PACS numbers: 03.65.-w, 02.30.Rz

I. INTRODUCTION

In quantum mechanics, there exist two parallel themes. One is about the static properties of a system, namely the eigenstates and eigenvalues of the Hamiltonian. Technically, in the nonrelativistic case, it is about the time-independent Schrödinger equation. The other is about the dynamics of the system, namely how the wave function or the expectation values of various physical quantities evolve. Technically, it is about the time-dependent Schrödinger equation. While for the former, there exist many theorems which give us a good picture of the wave functions in many cases; for the latter, the relevant mathematics is far less developed, and hence we often have little intuition. Actually, the dynamics of the system can turn out to be very surprising. This is the case even in the single particle case, as the celebrated phenomena of dynamical localization [1] and coherent destruction of tunneling [2] demonstrate.

In this paper, we report some unexpected dynamics in the setting of the one-dimensional tight binding model, which is arguably the simplest model in solid state physics. It is about a very simple scenario. We take a tight binding model with periodic boundary condition and put a particle in some eigenstate, i.e., a Bloch state with some momentum. Then suddenly we quench it by changing the potential of some site. The rough picture is that the particle will be reflected by the newly introduced barrier, and the particle will do Rabi oscillation between the initial Bloch state and its time-reversed counterpart. However, exact numerical simulation reveals the unexpected fact that the curves of some physical quantities like the probability of finding the particle in the initial state, are structured. Specifically, they show *cusps* periodically in time.

The cusps here are somehow similar to the cusps observed previously [3], which is also in the tight binding model setting (the cusps there were observed earlier in quantum optics settings [4, 5] but were not fully accounted for). However, the crucial difference is that, while there it is a perturbative effect and survives only in the weak driving limit, here it is a generic nonperturbative effect and thus is very robust.

In the following, we shall first describe the phenomenon

by presenting the numerical observations in Sec. II. Then in Sec. III we will identify the essential features of the underlying Hamiltonian, from which we define an idealized toy model. The phenomenon is then accounted for by solving the dynamics of the toy model analytically.

II. PERIODICALLY APPEARING CUSPS

The N -site tight binding model Hamiltonian is ($\hbar = 1$ throughout this paper)

$$\hat{H}_0 = - \sum_{n=0}^{N-1} (\hat{a}_n^\dagger \hat{a}_{n+1} + \hat{a}_{n+1}^\dagger \hat{a}_n). \quad (1)$$

Here \hat{a}_n^\dagger (\hat{a}_n) is the creation (annihilation) operator for a particle in the Wannier function $|n\rangle$ on site n . With the periodic boundary condition, the eigenstates are the well-known Bloch states $\langle n|k\rangle = \exp(i2\pi kn/N)/\sqrt{N}$. Here k is an integer defined up to an integral multiple of N .

Now consider such a scenario. Initially the particle is in the Bloch state $|k_i\rangle$. Suddenly, at time $t = 0$, the potential on site 0 is changed to U . That is, we add the term $\hat{H}_1 = U\hat{a}_0^\dagger\hat{a}_0$ to the Hamiltonian (1). As the wave function $\Psi(0) = |k_i\rangle$ of the particle is no longer an eigenstate of the new Hamiltonian, nontrivial evolution starts. Two quantities of particular interest are the survival probability and the reflection probability

$$P_i(t) = |\langle +k_i|\Psi(t)\rangle|^2, \quad P_r(t) = |\langle -k_i|\Psi(t)\rangle|^2, \quad (2)$$

which are, respectively, the probability of finding the particle in the initial Bloch state and the momentum-reversed Bloch state. Both quantities can be easily calculated numerically as in Fig. 1. There we show the numerical results of P_i and P_r as functions of time. The lattice is of size $N = 401$, and three different sets of values of (k_i, U) are investigated.

The most prominent feature of the curves is the cusps. In each panel of Fig. 1, the cusps are equally spaced in time. They appear simultaneously in the curves of P_i and P_r . Sometimes, the cusp in one of the two curves is not so clearly visible, but the corresponding one in the other curve is well shaped. Of all of the three panels, panel (b) is especially regular. Not only the cusps appear

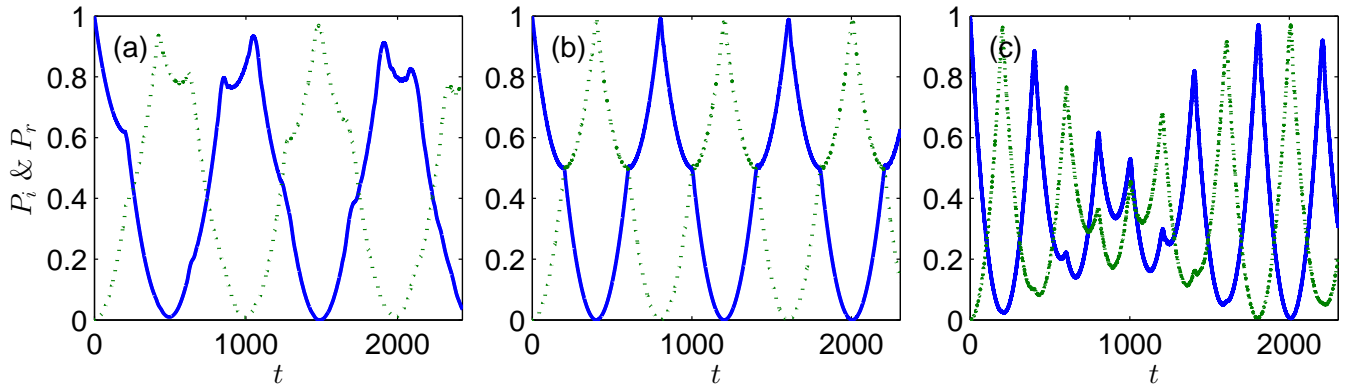


FIG. 1. (Color online) Time evolution of the probability of finding the particle in the initial Bloch state $|k_i\rangle$ (P_i , solid lines) and in the momentum-reversed Bloch state $|-k_i\rangle$ (P_r , dotted lines). Note that $P_i + P_r \neq 1$ in general as other Bloch states are occupied too. In all of the three panels, the size of the lattice is $N = 401$. The values of the parameters (k_i, U) are $(80, 1.5)$, $(100, 2)$, and $(100, 12)$ in (a), (b), and (c), respectively.

periodically, both curves are simply periodic. Moreover, when the cusps happen, $P_{i,r} = 0.5$ or 1 .

It is worthy to emphasize the essential difference between the cusps here and those observed previously in Ref. [3]. There it is a first order perturbative effect. The cusps exist only in the weak driving limit, or specifically, only when the survival probability (namely P_i) is close to unity, and between the cusps the survival probability is a linear function of time. In contrast, here apparently the cusps are still very sharp even when P_i constantly drops to zero. Moreover, the functional form of the curves between the cusps is neither linear nor, as we shall see below, exponential.

III. EXPLANATION BY A TRUNCATED AND LINEARIZED MODEL

To account for the cusps in Fig. 1, we need to have a close survey of the structure of the un-perturbed Hamiltonian \hat{H}_0 and perturbation \hat{H}_1 . Figure 2 shows the dispersion relation, $\varepsilon = -2 \cos q$ with $q = 2\pi k/N$, of \hat{H}_0 . The perturbation \hat{H}_1 couples two arbitrary Bloch states with an equal amplitude

$$g = \langle k_1 | \hat{H}_1 | k_2 \rangle = U/N, \quad (3)$$

regardless of the difference $k_1 - k_2$.

A crucial fact revealed by numerics is that in the evolution of the wave function, essentially only those few Bloch states with energy close to the energy $\varepsilon(q_i)$ of the initial Bloch state participate. Or in other words, only those Bloch states with $q \simeq \pm q_i$ contribute significantly to the wave function. Now since locally the dispersion curve $\varepsilon(q)$ can be approximated by a straight line (it is especially the case at $q_i = \pi/2$), we are led to truncate and linearize the model.

Of all the Bloch states, we retain only two groups centered at $|\pm k_i\rangle$. Each group consists of $2M + 1$ states

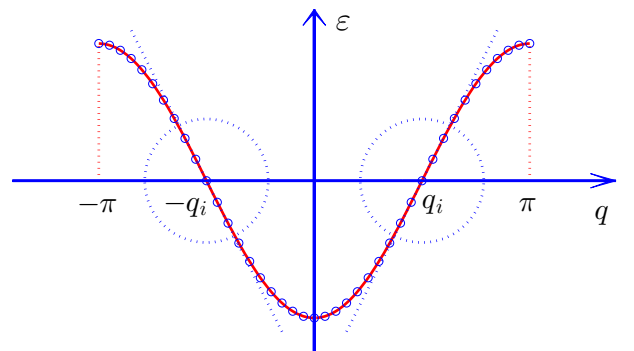


FIG. 2. (Color online) Dispersion relation $\varepsilon(q) = -2 \cos q$ of the tight binding model (1). The parameter $q_i = 2\pi k_i/N$ denotes the wave vector of the initial Bloch state. The dotted straight lines are local linear approximations to the dispersion curve. Only the Bloch states inside the circles participate significantly in the dynamics and thus are retained in the truncated Hamiltonian.

with wave numbers symmetrically distributed around k_i or $-k_i$. Let us now refer to them as $\{|R_n\rangle\}$ and $\{|L_n\rangle\}$, where R and L mean right-going and left-going, respectively, and n ranges from $-M$ to M . By choice, $|R_n\rangle = |k_i + n\rangle$ and $|L_n\rangle = |-k_i - n\rangle$. After linearizing the dispersion curve at $\pm q_i$, the energy of the degenerate states $|R_n\rangle$ and $|L_n\rangle$ is $n\Delta$, with $\Delta = 4\pi \sin q_i/N$. Again, the perturbation \hat{H}_1 couples two arbitrary states in the retained set of states with equal amplitude $g = U/N$.

This truncated and linearized model can be partially diagonalized by introducing a new basis as

$$|A_n^\pm\rangle = \frac{1}{\sqrt{2}}(|R_n\rangle \pm |L_n\rangle). \quad (4)$$

Referring to the original Hamiltonian \hat{H}_0 , they are even- and odd-parity states with respect to the defected site, respectively. It is easy to see that $|A_n^-\rangle$ are eigenstates of the total Hamiltonian $\hat{H} = \hat{H}_0 + \hat{H}_1$ with eigenvalues

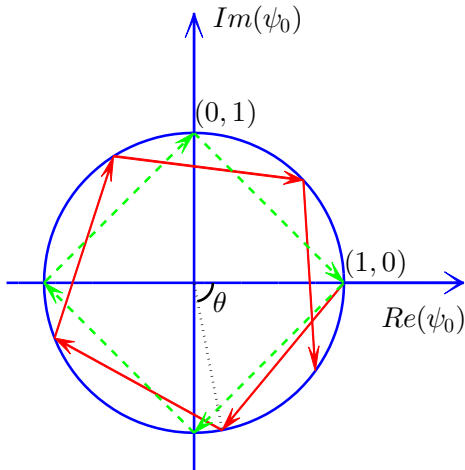


FIG. 3. (Color online) A generic (red solid lines) trajectory of ψ_0 on the complex plane according to Eq. (20). It is analogous to the bouncing of a ball inside a circular billiard. The green dashed closed trajectory corresponds to the case of $\theta = \pi/2$.

$n\Delta$. This is understood as that the odd-parity states do not feel the barrier at all. In the yet to be diagonalized subspace of $\{|A_n^+\rangle\}$, the matrix elements of \hat{H}_0 and \hat{H}_1 are

$$\langle A_n^+ | \hat{H}_0 | A_n^+ \rangle = n\Delta, \quad \langle A_{n_1}^+ | \hat{H}_1 | A_{n_2}^+ \rangle = 2g, \quad (5)$$

for arbitrary $n_{1,2}$.

Now the scenario is like this. Initially the system is in the level $|\Psi(0)\rangle = |R_0\rangle$. The problem is, how does the probability of finding the system in the initial level $|R_0\rangle$ evolve in time? We have the decomposition

$$|\Psi(0)\rangle = |R_0\rangle = \frac{1}{\sqrt{2}}|A_0^-\rangle + \frac{1}{\sqrt{2}}|A_0^+\rangle. \quad (6)$$

Since $|A_0^-\rangle$ is an eigenstate of \hat{H} , we see that at an arbitrary time later, the wave function has the form

$$|\Psi(t)\rangle = \frac{1}{\sqrt{2}}|A_0^-\rangle + \frac{1}{\sqrt{2}} \sum_{n=-M}^M \psi_n |A_n^+\rangle. \quad (7)$$

Here the initial value of ψ_n is $\delta_{n,0}$. The quantity wanted is $\psi_0(t)$, in terms of which the probabilities P_i and P_r are

$$P_i = \frac{1}{4} |1 + \psi_0|^2, \quad P_r = \frac{1}{4} |1 - \psi_0|^2. \quad (8)$$

The Schrödinger equation for the ψ 's is then

$$i \frac{\partial}{\partial t} \psi_n = n\Delta \psi_n + 2g \sum_{m=-M}^M \psi_m. \quad (9)$$

Note that the term in the summation is independent of n . Therefore, we define the collective quantity

$$S(t) = \sum_{m=-M}^M \psi_m(t). \quad (10)$$

The Schrödinger equation (9) can then be rewritten in the form

$$i \frac{\partial}{\partial t} \psi_n = n\Delta \psi_n + 2gS. \quad (11)$$

This equation can be easily solved by Duhamel's principle

$$\psi_n(t) = e^{-in\Delta t} \delta_{n,0} - i2g \int_0^t d\tau e^{-in\Delta(t-\tau)} S(\tau). \quad (12)$$

Plugging this into (10), we get an integral equation of S ,

$$S(t) = 1 - i2g \int_0^t d\tau \left(\sum_{n=-M}^M e^{-in\Delta(t-\tau)} \right) S(\tau). \quad (13)$$

Here we use some fact verified by numerics (see Figs. 4 and 5). Numerically, it is easy to find that as $M \rightarrow \infty$, the dynamics of the system converges quickly. Therefore, it is legitimate to replace the finite summation in the bracket by an infinite summation. That is,

$$S(t) \simeq 1 - i2g \int_0^t d\tau \left(\sum_{n=-\infty}^{+\infty} e^{-in\Delta(t-\tau)} \right) S(\tau). \quad (14)$$

Here we note that the infinite summation in the parentheses is periodic sampling of an exponential function, and thus, the famous Poisson summation formula applies [6]. We have

$$\sum_{n=-\infty}^{+\infty} e^{-in\Delta(t-\tau)} = T \sum_{n=-\infty}^{+\infty} \delta(t - \tau - nT), \quad (15)$$

where the period $T \equiv 2\pi/\Delta$. Substituting this into (14), we get

$$S(t) = 1 - i2gT \left(\frac{1}{2} S(t) \right), \quad (16)$$

for $0 < t < T$, by using the fact that $\int_0^\infty dt \delta(t) = 1/2$. We then solve

$$S(t) = \frac{1}{1 + igT}, \quad (17)$$

which is a constant, for $0 < t < T$. Substituting this into (12), we get

$$\psi_0(t) = 1 - \frac{i2gt}{1 + igT} = \frac{1 - i2g(t - T/2)}{1 + igT}, \quad (18)$$

which is linear in t . We note that as $t \rightarrow T^-$,

$$\psi_0(t) \rightarrow \frac{1 - igT}{1 + igT} = e^{-i\theta} \quad (19)$$

for some $\theta \in \mathbb{R}$. That is, after one period, ψ_0 returns to its initial value, except for a phase accumulated. This complete revival means, for $rT < t < (r+1)T$, the value of ψ_0 is

$$\psi_0(t) = \frac{1 - i2g[t - (r+1/2)T]}{1 + igT} e^{-ir\theta}. \quad (20)$$

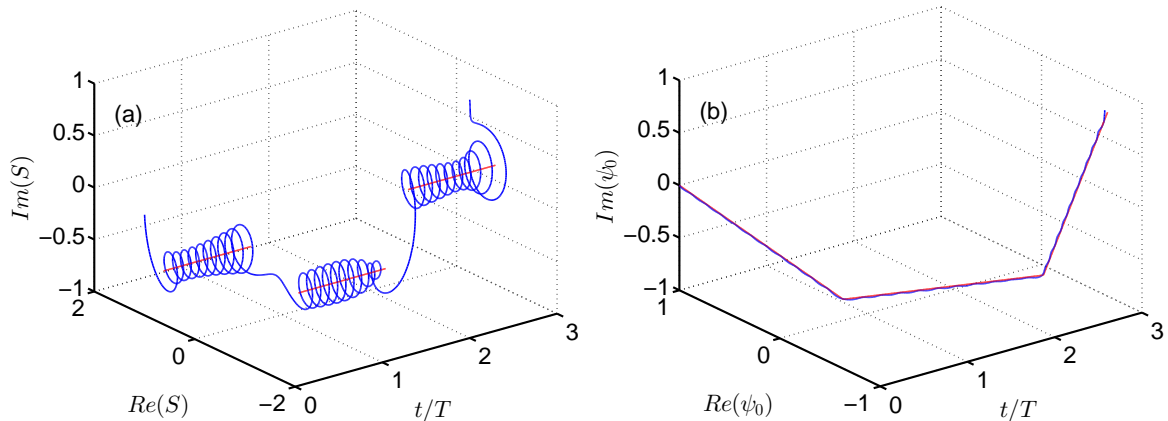


FIG. 4. (Color online) Time evolution (blue solid lines) of (a) the auxiliary quantity S and (b) ψ_0 for $M = 10$. In each panel, the red line indicates the analytical predictions of (23) or (20). Compare (b) with Fig. 3. The parameters are $\Delta = 1$, $g = 0.125$, and $T = 2\pi/\Delta$.

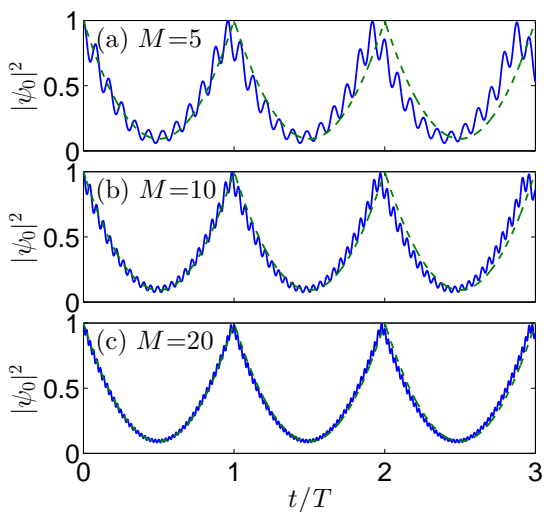


FIG. 5. (Color online) Time evolution of $|\psi_0|^2$ for a finite M . In each panel, the blue solid line indicates the numerical exact value while the dashed green line the analytical formula (20), which is valid in the $M \rightarrow \infty$ limit. In each period, the latter is a parabola. The parameters are $\Delta = 1$, $g = 0.5$, and $T = 2\pi/\Delta$.

We thus see that $|\psi_0|^2$ is a periodic function of time t . At $t = rT$, $r \in \mathbb{N}$, it returns to unity and in-between it is a quadratic function of t . In Fig. 3, the trajectory of ψ_0 on the complex plane is illustrated. It bounces inside the unit circle elastically like a ball.

Another way to derive (20) from (13) is as follows. Take the Laplace transform of both sides of (13). Let $L(p) = \int_0^\infty dt e^{-pt} S(t)$. We note that the integral on the right hand side of (13) is in the convolution form. Hence, we have the simple linear equation of $L(p)$,

$$L(p) = \frac{1}{p} - i2g \left(\sum_{n=-M}^M \frac{1}{p - in\Delta} \right) L(p). \quad (21)$$

In the limit of $M \rightarrow \infty$, by using Euler's identity of $\sum_{n \in \mathbb{Z}} 1/(z - n) = \pi \cot(\pi z)$ [7], we get

$$\begin{aligned} L(p) &= \frac{1/p}{1 + gT \cot(-ipT/2)} \\ &= \frac{1 - e^{-pT}}{(1 + igT)p} \sum_{r=0}^{\infty} e^{-r(i\theta + pT)}, \end{aligned} \quad (22)$$

where $e^{-i\theta}$ is defined as in (19). Then it is not difficult to see that

$$S(t) = \frac{1}{1 + igT} \sum_{r=0}^{\infty} e^{-ir\theta} \chi(rT < t < (r+1)T). \quad (23)$$

Here the characteristic function χ takes the value of unity if the condition in the parentheses is satisfied, and zero otherwise. We see that S takes a constant value in each interval of $(rT, (r+1)T)$. By (12) and (23), it is straightforward to get ψ_0 as in (20). Conversely, (23) is anticipated in view of (17) and (20).

A peculiar feature of (17) and (23) is that S is not continuous at $t = rT$. For example, by the definition (10), $S(t = 0) = \psi_0(t = 0) = 1$, however by (17), $S(t = 0^+) \neq 1$. This should be an artifact of our treatment involving the $M \rightarrow \infty$ limit. To see how this difficulty is solved for finite M , we demonstrate the typical time evolution behavior of S with $M = 10$ in Fig. 4(a). We see that in the interval of $rT < t < (r+1)T$, S oscillates rapidly around the constant value predicted by (23), and at about $t = rT$, the orbit of S quickly transits from around one constant value to around the next. Along with the time evolution of S in Fig. 4(a), we show in Fig. 4(b) the time evolution of ψ_0 . We see that the numerical exact value of ψ_0 follows the analytical prediction of (20) closely, with much smaller oscillation amplitude than S . This is reasonable in view of (12), where S appears in the integral and thus its oscillation is averaged out.

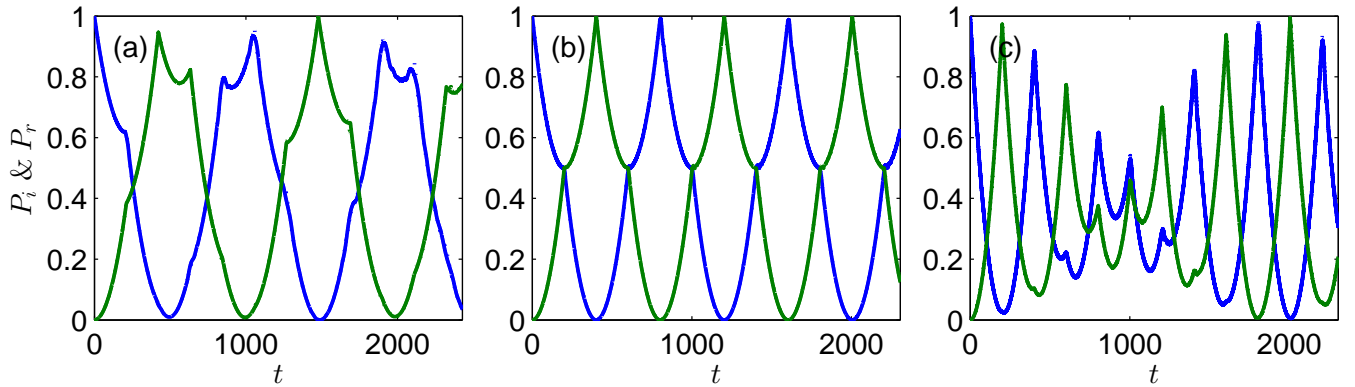


FIG. 6. (Color online) Comparison between the numerical exact values of $P_{i,r}$ and the analytical predictions. The panels correspond to those in Fig. 1 one to one and in order. The analytical curves are solid (respectively, dotted) if the corresponding numerical curves are dotted (respectively, solid). The dotted lines are hardly visible, which proves that the numerical and analytical results agree very well.

Further evidences demonstrating that the simple formula (20) is a good approximation for finite M (Anyway, there are only a finite number of levels in the original tight binding model) are presented in Fig. 5. There we see that even for $M = 5$, the formula (20) captures the behavior of $|\psi_0|^2$ on the scale of T very well, and as M increases, the curve converges to that predicted by (20) very quickly.

Having verified that (20) is reliable even for finite levels, we now apply the theory to the original problem. There we have $\Delta = 4\pi \sin q_i/N$ and $g = U/N$. Using (8) and (20), we can calculate $P_{i,r}$ in Fig. 1 analytically. The results are presented in Fig. 6 together with those numerical data in Fig. 1. We see that the analytical approximation and the numerical exact results agree very well. We can also understand the regularity of Fig. 1(b) now. For $U = 2$ and $q_i = \pi/2$, $gT = 1$ (regardless of the value of N) and hence $\theta = \pi/2$ and the trajectory of ψ_0 is the closed one in Fig. 3. By (8), it results in the regular behavior of $P_{i,r}$ in Fig. 1(b).

IV. CONCLUSION AND DISCUSSION

In conclusion, we have found the reflection dynamics of a Bloch state against a site defect to be nonsmooth. Specifically, the survival probability P_i and the reflection

probability P_r both show cusps periodically in time. This phenomenon is explained by analytically solving the dynamics of an idealized model retaining the essential features of the original tight binding model, namely, the locally equally spaced spectrum and the equal coupling between two arbitrary states.

The cusps are different on the one hand from those reported in Refs. [3–5] in that they are deeply non-perturbative, and on the other hand from those in Refs. [8–10] in that the functions in-between the cusps are not exponential but quadratic.

Although we do not believe the phenomenon reported here is universal, we do think it provides a good example demonstrating that the dynamics of a model, even the simplest one, can be very surprising. The point is that, thorough understanding of the static properties of a model (as we do for the model in question) does not imply thorough understanding of its dynamical properties. The former does not help much for the latter in many cases.

ACKNOWLEDGMENTS

We are grateful to M. Y. Ye, X. M. Lin, L. Chen, R. Y. Liao, F. Grossmann, and D. Braak for helpful discussions.

-
- [1] D. H. Dunlap and V. M. Kenkre, Phys. Rev. B **34**, 3625 (1986).
 - [2] F. Grossmann, T. Dittrich, P. Jung, and P. Hänggi, Phys. Rev. Lett. **67**, 516 (1991).
 - [3] J. M. Zhang and M. Haque, ScienceOpen Research 2014 (DOI: 10.14293/S2199-1006.1.SOR-PHYS.A2CEM4.v1).
 - [4] J. Parker and C. R. Stroud, Jr., Phys. Rev. A **35**, 4226 (1987).
 - [5] H. Giessen, J. D. Berger, G. Mohs, P. Meystre, and S. F. Yelin, Phys. Rev. A **53**, 2816 (1996).
 - [6] L. Grafakos, *Classical Fourier Analysis*, 2nd ed. (Springer-Verlag, New York, 2008).
 - [7] M. Aigner and G. M. Ziegler, *Proofs from THE BOOK*, 4th ed. (Springer-Verlag, Berlin, 2013).
 - [8] G. C. Stey and R. W. Gibberd, Physica (Amsterdam) **60**, 1 (1972).
 - [9] M. Ligare and R. Oliveri, Am. J. Phys. **70**, 58 (2002).

[10] W. Zhu and D. L. Zhou, arXiv:1507.02390.